Proteomic Evidence for Components of Spider Silk Synthesis from Black Widow Silk Glands and Fibers

Ro Crystal Chaw,*,† Sandra M. Correa-Garhwal,† Thomas H. Clarke,‡ Nadia A. Ayoub,‡ and Cheryl Y. Hayashi†

†Department of Biology, University of California, Riverside, California 92521, United States
‡Department of Biology, Washington and Lee University, Lexington, Virginia 24450, United States

S Supporting Information

ABSTRACT: Spider silk research has largely focused on spidroins, proteins that are the primary components of spider silk fibers. Although a number of spidroins have been characterized, other types of proteins associated with silk synthesis are virtually unknown. Previous analyses of tissue-specific RNA-seq libraries identified 647 predicted genes that were differentially expressed in silk glands of the Western black widow, *Latrodectus hesperus*. Only ∼5% of these silk-gland specific transcripts (SSTs) encode spidroins; although the remaining predicted genes presumably encode other proteins associated with silk production, this is mostly unverified. Here, we used proteomic analysis of multiple silk glands and dragline silk fiber to investigate the translation of the differentially expressed genes. We find 48 proteins encoded by the differentially expressed transcripts in *L. hesperus* major ampullate, minor ampullate, and tubuliform silk glands and detect 17 SST encoded proteins in major ampullate silk fibers. The observed proteins include known silk-related proteins, but most are uncharacterized, with no annotation. These unannotated proteins likely include novel silk-associated proteins. Major and minor ampullate glands have the highest overlap of identified proteins, consistent with their shared, distinctive ampullate shape and the overlapping functions of major and minor ampullate silks. Our study substantiates and prioritizes predictions from differential expression analysis of spider silk gland transcriptomes.

KEYWORDS: Ampullate silk glands, dragline silk, *Latrodectus hesperus*, mass spectrometry, silk fiber proteome, silk gland proteome, silk proteins, spider, spidroins, tubuliform glands
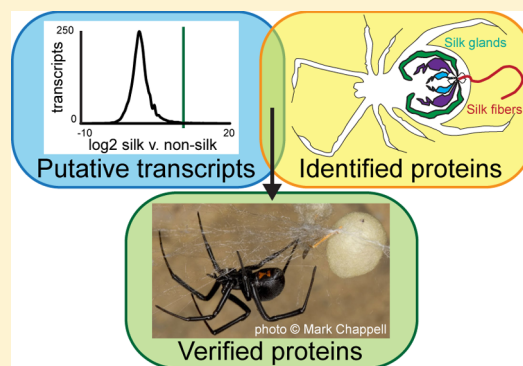
INTRODUCTION

Spider silks are renowned for their mechanical properties, but many aspects of how spiders produce these high-performance materials remain elusive. A spider's abdomen contains numerous silk glands that are differentiated into morphologically and functionally distinct types. Most gland types express members of a spider-specific gene family that encodes fiber-forming structural proteins called spidroins, a contraction of spider fibroins.[1,2] After synthesis, spidroins are stored in the lumen of silk glands as part of a liquid spinning dope. As needed, the dope travels through ducts leading to external spigots on the spider's spinnerets. During extrusion, the dope rapidly transitions from a liquid to a dry fiber.[1−4]

The mechanical properties of fibrous spider silks are related to the amino acid sequences of their spidroin components in that primary structure largely determines secondary and higher-level protein structures. Spidroins consist of iterated repeat units that vary in length and complexity depending on spidroin type. The significance of particular spidroin repeat sequences to fiber-specific mechanical properties has been demonstrated through a variety of structural studies.[5−8] Because of the direct relationship between spidroin amino acid sequences and the physical attributes of silk, characterization and recombinant expression of spidroins have been a main focus of spider silk research.[9−13]

Despite extensive spidroin research, knowledge of the gene expression and protein profiles that contribute to silk synthesis is far from complete. To further explore how spiders synthesize distinct silk types, the present study combines peptide analysis with transcriptomic data. The Western black widow spider, *Latrodectus hesperus*, produces six fibrous silk types from six corresponding silk gland types (major ampullate, minor ampullate, aciniform, flagelliform, pyriform, and tubuliform). Here, we focus on major ampullate, minor ampullate, and tubuliform silks. We chose these silk types because of the overlapping functions of major ampullate and minor ampullate silks in orb-weaving spiders,[14] the similar shapes of the major and minor ampullate glands, and evidence that the major ampullate and tubuliform silk glands share expression of some spidroin genes.[15,16]

Major ampullate silks emerge from major ampullate glands, which have a long tail that synthesizes proteins, an ampule-shaped sac that both synthesizes and stores proteins, and a Z-shaped duct that connects to an external spigot (Figure 1A).[17]
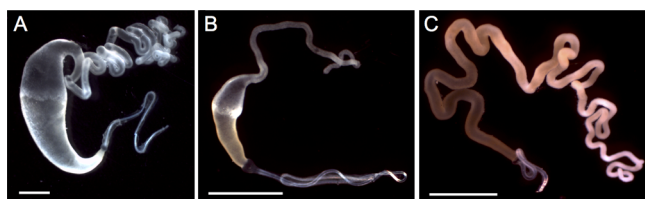
Figure 1. Bright-field images of *L. hesperus* silk glands: (A) major ampullate gland, (B) minor ampullate gland, and (C) tubuliform gland. (A, B) Anterior tail is at the top right, ampule-shaped lumen is to the left, and posterior Z-shaped duct is at the bottom right. (C) Anterior tail and posterior duct point toward the bottom right. Anterior tail is pale and to the right; posterior duct is darker and to the left. Scale bars are 1 mm.

Minor ampullate silks are produced from glands that are morphologically very similar to major ampullate glands but that are smaller, with a shorter tail and lower capacity sac (Figure 1B). The combination of a long tail, ampule-shaped lumen, and Z-shaped duct are unique to the major and minor ampullate silk glands.

L. hesperus major ampullate glands predominantly express the genes for two major ampullate spidroins (MaSp1 and MaSp2), and these proteins are the main components of *L. hesperus* dragline fibers.[15,16,18–20] Minor ampullate silk glands express minor ampullate spidroin (MiSp) genes, and MiSps are the primary proteins found in minor ampullate silks.[21,22] Minor ampullate silks are generally thought to be used by orb-weaving spiders as the auxiliary spiral during web construction and as support for major ampullate silks in draglines, web radii, and web scaffold.[14,21,22] In *L. hesperus,* which builds a cob-web instead of an orb-web, minor ampullate silks have been found in a composite of silk types used in prey wrapping.[23] Cob-webs are a derived type of orb-web,[24,25] and whether minor ampullate silks have any function during cob-web construction remains unknown. Their similar gland morphology and related silk functions suggest that major and minor ampullate spidroins have a close evolutionary relationship, but phylogenetic analysis of spidroins is inconclusive. For example, in Garb et al.,[15] MiSps tended to, but did not always, form a sister group to a large clade of MaSps.

In contrast to major and minor ampullate silks, the thick fibers that wrap *L. hesperus* egg cases are produced by glands that are unlike any other silk glands in shape: the elongated, worm-like tubuliform glands (also known as cylindrical glands; Figure 1C). The dominant transcripts in tubuliform glands encode tubuliform spidroins (TuSp1) and a family of silk proteins unrelated to spidroins, egg-case proteins (ECPs).[26–30] Despite having different shapes and producing functionally distinct silks, major ampullate and tubuliform silk glands are known to have overlapping spidroin gene expression. Major ampullate glands are dominated by *MaSp1* and *MaSp2* gene expression, but a 3′ tag profiling study of transcripts from *L. hesperus* major ampullate glands found expression of the tubuliform spidroin gene, *TuSp1*.[16] The converse is also true: *MaSp1* and *MaSp2* transcripts were present in *L. hesperus* tubuliform silk gland cDNA libraries.[15] It remains unknown, however, if the presence of nondominant spidroin transcripts in

silk glands unequivocally indicates their translation and whether the protein products are incorporated into silk fibers.

Tubuliform and major ampullate silk glands each express nonspidroin silk-related genes. ECPs are members of a nonspidroin gene family that were initially identified in black widow tubuliform glands and fibers and are thought to cross-link with TuSp1.[28] Further research has also found ECP homologues in a spider species without tubuliform glands, suggesting that ECPs have functions across multiple silk types.[31] The recently characterized low-molecular-weight cysteine-rich proteins (CRPs) are another category of non-spidroin silk constituents. CRPs appear in *L. hesperus* major ampullate glands and fibers and are thought to cross-link with MaSp1 and MaSp2 to increase silk fiber toughness.[32] Other nonspidroin proteins that are vital to the process of synthesizing and assembling spidroins must exist in each gland type, but these are currently unknown.

Deep transcriptome sequencing studies have made it possible to explore the gene expression profiles of silk glands and to address the dearth of nonspidroin, silk-related genes.[16,33–35] A substantial advance to understanding spider silk synthesis was the identification of 647 silk-gland specific transcripts (SSTs) from *L. hesperus* by Clarke et al.[34] SSTs are transcripts that were found to be significantly differentially expressed and at least 630 times more abundant in silk glands compared to that in nonsilk gland control tissues. Hence, SSTs are promising candidates for roles in spidroin production and fiber assembly. Previous mass spectrometry studies of protein extracts from *L. hesperus* egg case wrapping, attachment discs, and gland luminal contents has demonstrated the translation of seven types of silk structural proteins encoded by SSTs (aciniform spidroin, ECPs, minor ampullate spidroin, major ampullate spidroins 1 and 2, tubuliform spidroin, and pyriform spidroin).[23,28,29,36,37] It remains unknown whether all or only some of the remaining SSTs are translated into proteins.

In the present study, we use peptide sequencing to generate protein profiles for the major ampullate, minor ampullate, and tubuliform silk glands as well as the major ampullate fiber of *L. hesperus*. From these proteomes, we identify proteins arising from the SSTs. The SSTs identified by Clarke et al.[34] are from the combined set of *L. hesperus* silk glands, which makes their localized expression among gland types impossible to discern. Knowing which SSTs are translated in different glands will identify SSTs that are necessary for general silk gland functions (protein products in multiple gland types) and SSTs that are necessary for the synthesis and storage of specific silks (protein products restricted to one gland type). Additionally, if an SST protein product appears in both the major ampullate gland and fiber, then it may have utility in silk fiber assembly or function rather than having exclusive importance in the gland-specific functions of producing and maintaining silk protein reserves.

We predict that major and minor ampullate glands will have similar proteomes, consistent with their similar shape and the overlapping functions of major and minor ampullate silks. We also expect that tubuliform glands will contain TuSp1 and ECPs and that major ampullate glands will contain MaSp1, MaSp2, and CRPs. Tubuliform glands may also express MaSp1 and MaSp2, which would be consistent with the discovery of *MaSp1* and *MaSp2* transcripts in tubuliform gland cDNA, and, conversely, major ampullate glands may express TuSp1, consistent with the detection of *TuSp1* transcripts in major ampullate glands.[15,16] Comparing major ampullate glands to major ampullate fibers, we expect that only a small subset of the

SST protein products identified in major ampullate glands will appear in the fiber. This subset should contain MaSp1, MaSp2, and CRPs.

The goal of this research is to combine hypothetical gene products predicted by *de novo* assembled RNA-seq data[34] with proteomic data to gain a broader understanding of how spiders generate silk *in vivo*. This analysis will extend the framework on how silk dope and fibers are generated by spiders and of gene products that are exceptional candidates for involvement in the synthesis of spider silk.

■ MATERIALS AND METHODS

Animal Collection, Dissection of Silk Glands, and Collection of Silk Fibers

Adult *L. hesperus* females were collected on the University of California, Riverside, campus and were fed commercially available crickets. Prior to dissection, individuals were not fed for 2 days to minimize contamination from gut contents. Spiders were individually anesthetized using carbon dioxide gas, and their abdomens were dissected in 1× SSC. In *L. hesperus*, major ampullate, minor ampullate, and tubuliform glands are easily distinguished during dissection because of their distinctive morphologies and spatial arrangement in the abdomen (Figure 1).[38] Silk glands were visually inspected to ensure that there were no breaks or punctures. If damage was detected, no silk glands from that individual were used to avoid cross-contamination. Major ampullate, minor ampullate, and tubuliform glands were dissected into separate microfuge tubes and flash frozen in liquid nitrogen or immediately used for protein extraction (below).

Major ampullate silk fibers were manually drawn from spiders as described in the literature.[32,39] Major ampullate fibers are extruded from large and distinctive silk spigots, enabling visual verification of major ampullate silk collection during fiber harvesting.[32] Fibers were drawn onto spools at a rate of 5−7 cm per second for a total of 2−3 min. It was sometimes necessary to use up to three individuals to amass the targeted amount of silk fibers. Fibers from each individual were stored on separate spools at room temperature in closed containers.

Two biological replicates were collected for each gland type and major ampullate silk fibers. Replicates consisted of one of the following: two major ampullate glands from one individual, six tubuliform glands from one individual, four minor ampullate glands from two individuals, or the combined silk spools of up to three individuals.

Protein Extraction

Fresh or frozen silk glands were macerated with a sterile pestle in protein extraction buffer (10% glycerol, 50 mM Tris, pH 7.5, 5 mM $MgCl_2$, 2% SDS, 150 mM NaCl, 0.2% β-mercaptoethanol, 0.005 M EDTA) supplemented with Halt protease inhibitor cocktail (Thermo Fisher Scientific, Waltham, MA). Silk fibers were cut with a clean razor blade, immersed in protein extraction buffer supplemented with Halt protease inhibitor cocktail, macerated with a sterile pestle, and incubated at room temperature overnight. Samples were then fractionated on an SDS-PAGE gel (5% stacking and 6.4% separating) and visualized with Bio-Safe Coomassie stain (Bio-Rad, Hercules, CA). Protein concentrations were estimated from these visualizations, with a target of ≥500 ng/lane. For each sample, multiple lanes (10−15 μL/lane; total of 20−30 μL of sample) were excised and combined for in-gel digest (Supporting Information Figure S1).

Standard protocols for in-gel tryptic digestion from the Arizona Proteomics Consortium (http://proteomics.arizona.edu/protocols) were followed. Briefly, proteins in acrylamide gels were digested overnight at 37 °C with 12.5 ng/μL trypsin and 1.25 ng/μL chymotrypsin in 50 mM ammonium bicarbonate with 10 mM calcium chloride. Digested peptides were extracted from gel pieces with a Bioruptor Standard sonication system (Diagenode, Denville, NJ) for 30 min. After sonication, the supernatant was purified using Ziptips C_{18} pipette tips according to the manufacturer's instructions (Millipore, Billerica, MA), dried, and stored at −20 °C until shipment for analysis at the Arizona Proteomics Consortium.

LC−MS/MS Analysis

LC−MS/MS analysis of trypsin/chymotrypsin-digested proteins was carried out using a LTQ Orbitrap Velos mass spectrometer (Thermo Fisher Scientific) equipped with an Advion nanomate ESI source (Advion, Ithaca, NY). Peptides were eluted from a C18 precolumn (100 μm i.d. × 2 cm, Thermo Fisher Scientific) onto an analytical column (75 μm i.d. × 10 cm, C18, Thermo Fisher Scientific). Solvent A was 0.1% formic acid in water. Solvent B (acetonitrile, 0.1% formic acid) was used for the following concentrations and times: 5%, 5 min; 5−7%, 5 min; 7−15%, 45 min; 15−35%, 60 min; 35−40%, 28 min; 40−85%, 5 min; 85%, 10 min; a return to 5% in 1 min, and another 10 min hold of 5% solvent B. All flow rates were 400 nL/min. Certain LC−MS/MS replicate runs were also performed using a shorter 125 min RP gradient (5% solvent B hold for 10 min; 5−20%, 65 min; 20−35%, 25 min; 35%, 9 min; 35−95%, 5 min; and finally a 95% solvent B hold for another 5 min).

Data Analysis

Data-dependent scanning was performed by Xcalibur, v 2.1.0, software[40] using a survey mass scan at 60 000 resolution in the Orbitrap analyzer scanning mass/charge (m/z) 400−1600, followed by collision-induced dissociation (CID) tandem mass spectrometry (MS/MS) of the 14 most intense ions in the linear ion trap analyzer. Precursor ions were selected by the monoisotopic precursor selection (MIPS) setting, with selection or rejection of ions held to a ±10 ppm window. Dynamic exclusion was set to place any selected m/z on an exclusion list for 45 s after a single MS/MS.

Tandem mass spectra were searched against a protein database made by combining Chelicerata proteins downloaded from NCBI on October 17, 2013 and reduced for redundant entries via CD Hit (available at http://weizhong-lab.ucsd.edu/cd-hit/) with common contaminant proteins such as keratins (ftp://ftp.thegpm.org/fasta/crap/) and with a nonredundant longest open reading frame translation of an *L. hesperus* transcriptome (Clarke et al.;[34] see above). At the time of the search, this combined protein database contained 182 000 entries. All MS/MS spectra were searched against the protein database described above using Thermo Proteome Discoverer 1.3 (Thermo Fisher Scientific) considering tryptic/chymotryptic peptides with up to 2 missed cleavage sites. Iodoacetamide derivatives of cysteines and oxidation of methionines were specified as variable modifications. Proteins were identified at 99% confidence with XCorr score cutoffs, as determined by a reversed database search.[41] The protein and peptide identification results were visualized with Scaffold, v 3.6.1 and v 4.0 (Proteome Software Inc., Portland, OR), a program that relies on various search engine results (i.e., Sequest, X!Tandem, MASCOT) and that uses Bayesian

statistics to reliably identify more spectra.[42,43] Proteins were accepted that passed a minimum of two peptides identified at 95% peptide confidence and 99.9% protein confidence by the Peptide and Protein Profit algorithms, respectively, within Scaffold.

Sample reports were exported from Scaffold. Contaminants were removed prior to further analysis. The similarities among the identified protein sets from each sample were quantified in R using the APE package[44,45] via a binary character matrix, with observed protein presence within a library (protein identification probability >95%) as the positive result. From the matrix, we calculated the distances between protein libraries using Simple Matching,[46] from which we built a dendrogram via hierarchical clustering.[44] Support for the dendrogram was calculated via bootstrapping with 10 000 replications using a custom R script.

Replicates were collapsed by taking the higher protein identification probability of the two replicates from the Scaffold analysis. The list of identified proteins included SSTs. Because an SST was not always the top protein identified, we further examined the identified NCBI proteins to see if they were associated with SSTs. To do this, we used the identified NCBI nr proteins to build a custom BLAST database. We searched this database with the longest open reading frame non-redundant translation of the *L. hesperus* transcriptome in a BLASTp search.[34] Up to five results with an *e*-value less than 1×10^{-5} for each query sequence were retained. The most relevant SST from the set of BLAST hits was determined by searching for presence of peptide sequences. SST UniProt annotations were taken from Clarke et al.[34] Sequences for CRP1−5 were obtained from Pham et al.[32] CRPs were identified with a BLASTp search against the longest open reading frame translation of the *L. hesperus* transcriptome using an *e*-value cutoff of 1×10^{-5}.[34]

■ RESULTS AND DISCUSSION

The Proteomes of Major and Minor Ampullate Glands Are the Most Similar

We identified 842 putative proteins in the major ampullate, minor ampullate, and tubuliform glands of *L. hesperus* (Scaffold sample report; Supporting Information File S1). The protein identifications in tubuliform gland biological replicates clustered together in a well-supported group (dendrogram bootstrap support = 100%; Supporting Information Figure S2). Major ampullate gland biological replicates also clustered with each other (dendrogram bootstrap support = 92%; Supporting Information Figure S2). One minor ampullate gland replicate grouped more tightly with the major ampullate gland replicates (bootstrap = 88%; Supporting Information Figure S2) than it did with the other minor ampullate gland replicate.

The difference between the minor ampullate gland replicates may be due to concentration-based variability in detectable proteins. Minor ampullate glands are, at most, approximately one-third the length of the other gland types used in this study, and glands from multiple individuals were combined in a single replicate to achieve target concentrations (Figure 1; see Materials and Methods). The detectable proteins between the replicates may differ because of variation in protein expression among individuals. Despite differences between the minor ampullate gland replicates, consistent with shared ampullate shapes, both minor ampullate gland biological replicates formed a group with the major ampullate gland replicates (bootstrap

support = 91%; Supporting Information Figure S2), with tubuliform gland replicates being more differentiated.

The subsets of identified proteins that correspond to SSTs also show greater similarity between major ampullate and minor ampullate glands than to tubuliform glands. Of the 647 SSTs from Clarke et al.,[34] 48 were predicted by peptide matches in major ampullate, minor ampullate, and tubuliform gland protein extractions (Supporting Information File S2). Some of the identified proteins were fragments from different regions of the same protein; therefore, the total number of unique proteins predicted by peptide matches to SSTs was 39 (Figure 2 and Supporting Information File S2). Out of these 39, only 28 had UniProt hits with an *e*-value less than 1×10^{-5}.

Twenty-four unique predicted proteins that matched SSTs were identified from major ampullate glands, 24 from minor ampullate glands, and 14 from tubuliform glands (Figure 2). Fifteen SST encoded proteins were found in two gland types. The major and minor ampullate glands had 13 SST encoded proteins in common. The major ampullate and tubuliform glands had one SST encoded protein in common that was not found in the minor ampullate gland, and minor ampullate and tubuliform glands also had one in common that was not observed in the major ampullate gland. Four SST encoded proteins were found in all gland types (Figure 3). In dendrogram analyses of sample replicates, the subset of SST encoded proteins grouped by gland type (minor ampullate bootstrap support = 85%, major ampullate bootstrap support = 91%, tubuliform bootstrap support = 100%; Supporting Information Figure S3). Minor ampullate gland replicates grouped with the major ampullate gland replicates (bootstrap support = 88%; Supporting Information Figure S3).

The higher amount of overlap between the SST protein profiles from major and minor ampullate glands reflects their comparable gland morphologies and silk functions (Figures 1−3 and Supporting Information Figure S3). These findings are also consistent with phylogenetic analyses of the spidroin family that showed a large clade of MaSps as most closely related to MiSps and that TuSp1 is more closely related to non-MiSp prey-swathing silk proteins (aciniform spidroin, AcSp1).[15] Thus, multiple sources of evidence (proteomic profiling of silk glands, morphology of silk glands, and evolutionary relationships of spidroins associated with particular silk glands) support the close evolutionary and functional relationship of major and minor ampullate spidroins as well as the similar morphologies of major and minor ampullate glands.
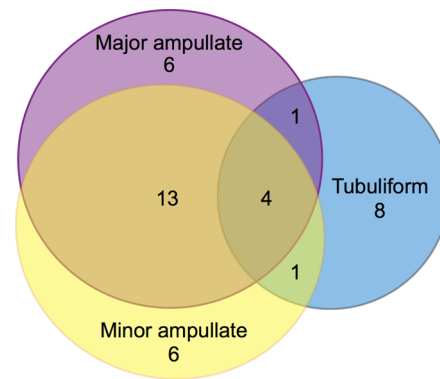
Major Ampullate, Minor Ampullate, and Tubuliform Silk Glands Contain a Variety of SST Proteins

Nine previously characterized silk-related proteins were identified among the 39 SST proteins (9/39; 23%; Figure 2). As expected, MaSp1, MaSp2, and CRP1 were identified in major ampullate silk glands, MiSp, in minor ampullate silk glands, and TuSp1 and ECP1, in tubuliform silk glands. CRP1 was exclusively observed in major ampullate glands. MiSp was identified only from minor ampullate glands, and TuSp1 and ECP1 were found solely in tubuliform glands. In contrast, MaSp1 was identified from all three glands, and MaSp2 was found in both major and minor ampullate glands. Major ampullate silk transcripts and proteins have not previously been documented in minor ampullate silk glands. The expression of major ampullate spidroins in minor ampullate glands could be due to similarities in their genetic programs, mirroring their shape and functional similarities.
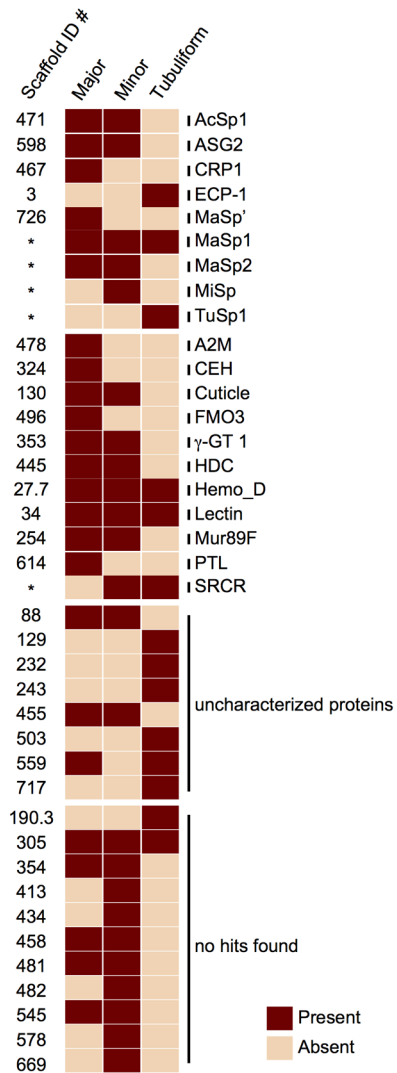
Figure 2. Chart of presence (red) or absence (light orange) of peptide-predicted proteins encoded by SSTs. Predicted proteins from *L. hesperus* major ampullate, minor ampullate, and tubuliform silk glands with best UniProt hits $<1 \times 10^{-5}$ are shown. Proteins are arranged alphabetically by name within groups: silk structural proteins, other characterized proteins, uncharacterized proteins, and proteins with no UniProt hits. *, protein type has more than one predicted protein. Abbreviations: A2M, alpha-2 macroglobulin; Ac, aciniform; ASG, aggregate spider glue; CEH, carboxylic ester hydrolase; CRP, cysteine rich protein; Cuticle, cuticle protein; ECP, egg case protein; FMO3, dimethylaniline monooxygenase; GT, glutamyltranspeptidase; HDC, histidine decarboxylase; Hemo_D, hemocyanin subunit D; Lectin, putative lectin; Ma, major ampullate; Mi, minor ampullate; Mur89F, mucin related 89F; Scaffold ID no., Scaffold predicted protein number; Sp, spidroin; Tu, tubuliform.

The discovery of MaSp1 proteins in tubuliform silk glands is consistent with previous studies that identified *MaSp1* transcripts from tubuliform silk gland cDNA libraries.[26] However, contrary to previous observations of *MaSp2* transcripts in tubuliform silk glands and *TuSp1* transcripts in major ampullate silk glands, we identified neither MaSp2 proteins in tubuliform silk glands nor TuSp1 proteins in major ampullate glands.[16,26] Little is known about regulation of spidroin expression and translation, and our results suggest complicated translational control of silk structural proteins.

Figure 3. Euler diagram[47] showing numbers of unique and shared predicted SST proteins in *L. hesperus* major ampullate (purple), minor ampullate (yellow), and tubuliform (blue) silk glands. Ellipses areas and overlap areas are proportional to the number of unique and shared proteins in and between gland types.

Unexpectedly, we found two other known silk-related proteins, aciniform spidroin and an aggregate spider glue (AcSp1 and ASG2, respectively) in the major and minor ampullate glands (Figure 2). A previous investigation that used 3′ tag profiling of RNA transcripts from major ampullate glands did not report the presence of *AcSp1* or *ASG2* transcripts.[16] If *AcSp1* is a rare transcript, then the focus on highly differentially expressed 3′ tags in Lane et al.[16] may explain the discrepancy with our results. *L. hesperus AcSp1* is an exceptionally large molecule (>19 kb) with a lengthy repetitive region flanked by relatively short amino (N)- and carboxyl (C)-terminal regions.[36,48] In our analysis, the protein identified as AcSp1 (Scaffold ID no. 471; Figure 2) has peptide matches to the N-terminal and repetitive regions. Rare transcript expression would mean that there are few 3′ terminal regions available for tagging, whereas enzyme digested AcSp1 protein would result in many protein fragments detectable by peptide analysis. An alternative explanation is that the two individuals in the 3′ tag profiling study were not expressing *AcSp1* transcripts at the time of RNA extraction. This explanation suggests that ampullate glands may transiently express *AcSp1* and that accumulated AcSp1 protein could be detectable with proteomic approaches.

ASG2 is a putatively glycosylated protein secreted as part of sticky droplets involved in prey capture.[49] ASG2 transcripts and proteins have not previously been detected in major and minor ampullate glands. Our finding may be indicative of the specific uses of ampullate silks by black widows. In orb-web weaving spiders, major ampullate silk is used as dragline and as the web frame and radii, and minor ampullate silks are used as temporary spiral during web construction. In black widows, major ampullate silks are thought to be the core fiber of the "gumfooted" lines that stick to and entangle prey.[50,51] After ensnarement, minor ampullate silks are incorporated into a composite of different silk types for prey restraint.[23] Given the function of major and minor ampullate silks in *L. hesperus,* black widow ampullate-shaped silk glands may additionally synthesize prey capture glue proteins such as ASG2.

In the major ampullate gland, peptides identified the translation of an SST sequence that we refer to as MaSp′ to distinguish it from MaSp1 and MaSp2 (Figure 2, Scaffold ID no. 726). The MaSp′ peptide matches are unique to an SST with a top UniProt hit to MaSp1 (Supporting Information File S2), but the sequence is distinct from either MaSp1 or MaSp2.

The SST that encodes MaSp′ appears to be a newly discovered member of the spidroin gene family, and its translation into a protein indicates that MaSp′ is functional.

Other than known silk-related proteins, 11 SST translations with characterized UniProt protein matches were detected in the ampullate glands. Four were exclusive to the major ampullate gland, four were identified in the major ampullate and minor ampullate glands, one was found in the minor ampullate and tubuliform glands, and two were in all glands (Figure 2). The four proteins exclusive to the major ampullate gland were three enzymes and a protein that have been described in vertebrates (abbreviation, SST to UniProt e-value): alpha-2 macroglobulin (A2M, 0), carboxylic ester hydrolase (CEH, 6×10^{-107}), dimethylaniline monooxygenase (FMO3, 7×10^{-147}), and putative triacylglycerol lipase (PTL, 3×10^{-43}). Because they are exclusive to major ampullate silk glands, A2M, CEH, FMO3, and PTL are candidates for having specific roles in the synthesis of major ampullate silks.

Five UniProt annotated SST proteins beyond silk structural proteins were associated with two gland types (Figure 2). Major and minor ampullate glands shared four proteins: putative cuticle protein (Cuticle, 2×10^{-20}), putative gamma glutamyltranspeptidase-1 (γ-GT-1, 4×10^{-152}), histidine decarboxylase (HDC, 0), and mucin related protein 89F (Mur89F, 2×10^{-11}). Minor ampullate and tubuliform silk glands contained one protein in common: scavenger receptor cysteine-rich protein (SRCR; 1×10^{-100}). Cuticle proteins have previously been described in spider silk gland ducts,[52] but the other proteins are undescribed in spiders. On the basis of the glands in which they were found, these five proteins may be involved in either functions exclusive to ampullate glands (Cuticle, γ-GT-1, HDC, Mur89F) or functions that are more general to different silk gland types (SRCR).

Two non-silk-related SST proteins were found in all three silk gland types. These were an oxygen transport molecule and a carbohydrate binding protein: hemocyanin subunit D (Hemo_D, 0) and a putative lectin (Lectin, 6×10^{-163}), respectively. Because of their detection in the three silk glands, these proteins may be common to other types of spider silk glands, such as aciniform, pyriform, and flagelliform.

Major Ampullate Fibers Have a Diverse Proteomic Profile

Analysis of protein extractions from major ampullate glands and fibers resulted in 527 protein predictions (Scaffold samples report is Supporting Information File S3). Of the 527 proteins, 86 were found in the fiber (Supporting Information File S3). Twenty-nine of the 527 proteins had SST encoded protein matches, with 17 in the fiber (Supporting Information File S4). Only nine of the 29 were unique to this major ampullate gland and fiber analysis; the remaining SST encoded proteins overlapped with those identified in the three-gland analysis of major ampullate, minor ampullate, and tubuliform silk glands. Some of the 29 SST predicted proteins were fragments of the same protein; thus, we identified a total of 25 unique putative proteins (Figure 4 and Supporting Information File S4). These fell into four groups: six matched silk structural proteins, nine were other characterized proteins, three were uncharacterized, and seven had no hits in the UniProt database (Figure 4 and Supporting Information File S4). CRP1 was identified and considered a silk structural protein (Figure 4, Scaffold ID no. 165, and Supporting Information File S4).

We predicted that major ampullate fiber SST matches would be a subset of the gland SST matches. Indeed, of the 25 unique
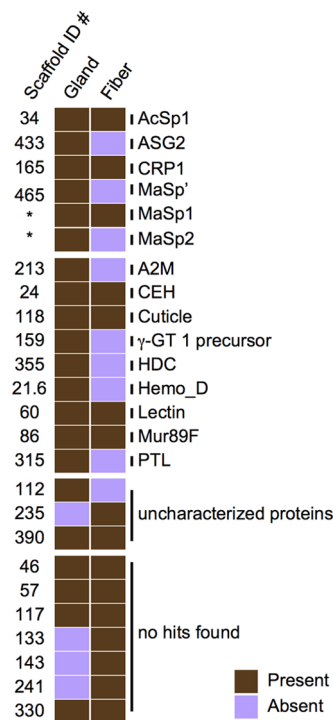
Figure 4. Chart of presence (brown) or absence (purple) of peptide-predicted proteins encoded by SSTs from *L. hesperus* major ampullate silk glands and fibers. Proteins are arranged alphabetically by name of best UniProt hits $<1 \times 10^{-5}$ within groups: silk structural proteins, other characterized proteins, uncharacterized proteins, and proteins with no UniProt hits. *, protein type has more than one predicted protein. Abbreviations: A2M, alpha-2 macroglobulin; Ac, aciniform; ASG, aggregate spider glue; CEH, carboxylic ester hydrolase; CRP, cysteine-rich protein; Cuticle, cuticle protein; FMO3, dimethylaniline monooxygenase; GT, glutamyltranspeptidase; HDC, histidine decarboxylase; Hemo_D, hemocyanin subunit D; Lectin, putative lectin; Ma, major ampullate; Mi, minor ampullate; Mur89F, mucin related 89F; PTL, pancreatic triacylglycerol lipase; Scaffold ID no., Scaffold predicted protein number; Sp, spidroin.

predicted SST proteins, 12 were found in the fiber and the gland, nine were exclusive to the gland, and four were exclusive to the fiber (Figure 4 and Supporting Information File S4). We did not expect to find any proteins exclusive to the fiber because the fiber is a product of the gland. One of the fiber-exclusive SST proteins matched an uncharacterized UniProt protein, and the remaining three had no hits in the UniProt database. These four fiber-exclusive SST encoded proteins may have been present in the gland, but they were difficult to detect because the gland has a greater variety of proteins than that in the fiber. In addition, the possibility of contamination of major ampullate fibers with products from other silk glands can never be entirely dismissed despite our use of microscopic observation while collecting fibers.

Consistent with our results from the three-gland analysis, we identified the expected MaSp1, MaSp2, and CRP1 in the major ampullate gland and we also found AcSp1, ASG2, and MaSp′. Three of these silk structural proteins were identified in the fiber: AcSp1, CRP1, and MaSp1. Incorporation of AcSp1 into draglines has not previously been documented. Discovery of AcSp1 protein in the fiber confirms the protein matches to AcSp1 in ampullate glands (Figures 2 and 4). Similarly, the presence of CRP1 and MaSp1 is consistent with previous peptide studies of *L. hesperus* major ampullate glands and fibers.

However, we also expected MaSp2 to be incorporated into the dragline.[15,16,18−20,32] The nondetection of MaSp2 may be due to a greater proportion of MaSp1 in the fiber. The relative proportions of MaSp1 and MaSp2 varies in draglines, and previous evidence suggests a more than 2-fold greater abundance of MaSp1 compared to that of MaSp2 in *L. hesperus* major ampullate fibers (2.5:1 ratio of MaSp1 to MaSp2).[20] Alternatively, the lack of MaSp2 detected in the fiber could be due to poor solubility of this spidroin, hampering its inclusion in the protein digests.

We also identified several non-silk-related protein products. Of the nine SST proteins with UniProt matches that were not silk-related, four were identified in both glands and fibers and five were exclusive to the gland. The four in both glands and fibers were also previously identified in the three-gland analysis: CEH, cuticle, lectin, and Mur89F. The identification of these four proteins in major ampullate fibers suggests that they may be crucial to fiber assembly or function.

CONCLUSIONS

We identified 48 SST encoded proteins in our three-gland analysis and nine additional SST encoded proteins in the major ampullate gland and fiber analysis (Supporting Information Files S2 and S4). Thus, we provide evidence for translation of 9% (57/647) of the SSTs from Clarke et al.[34] These included known silk-related, non-silk-related, and uncharacterized proteins. We show that silk structural genes that are not known to have dominant expression in a given gland type are translated and that some of these nondominant proteins are incorporated into draglines (e.g., AcSp1). Peptide analysis also demonstrates translation of putative enzymes, cuticle, and lectin proteins and 18 predicted proteins encoded by SSTs that had no UniProt hit.

These findings provide clues about the evolutionary history of spider silk types and suggest new ways that spiders may vary silk properties. We demonstrate similarity between proteomes of major and minor ampullate glands. This result is consistent with the differentiation of major and minor ampullate glands from a more generalized ampullate gland type. We also show that minor ampullate glands contain MaSp1 and MaSp2 and that AcSp1 is present in dragline silk fibers. Inclusion of MaSp1 and MaSp2 in minor ampullate silk fibers and inclusion of AcSp1 in draglines could modulate the tensile properties of silk fibers. Similarly, the expression of ASG2 glue proteins in *L. hesperus* ampullate glands may improve the utility of ampullate silks for prey capture by altering major and minor ampullate silk properties. Overall, our proteomic analysis combined with RNA-seq-derived transcript predictions provides greater insight into the evolution and synthesis of spider silks.

ASSOCIATED CONTENT

Supporting Information

The Supporting Information is available free of charge on the ACS Publications website at DOI: 10.1021/acs.jproteome.5b00353.

> Coomassie-stained gel images and dendrograms (PDF). Scaffold sample reports with clusters from peptide analysis and SST encoded predicted proteins from *L. hesperus* for major ampullate, minor ampullate, and tubuliform glands and silk fibers (XLSX).

The mass spectrometry proteomics data have been deposited to the ProteomeXchange Consortium[53] via the PRIDE partner repository. The data set for the analysis of three silk gland types has the data set identifiers PXD002595 and 10.6019/PXD002595. The data set for the major ampullate gland and fiber analysis has the data set identifiers PXD002592 and 10.6019/PXD002592.

AUTHOR INFORMATION

Corresponding Author

*E-mail: rcrystal@ucr.edu; Phone: 951-827-7323; Fax: 951-827-4286.

Author Contributions

R.C.C. collected and analyzed data and drafted the manuscript. S.M.C.-G. collected and analyzed data. T.H.C. and N.A.A. contributed to data analyses. C.Y.H. conceived the study, contributed to data analyses, and drafted the manuscript. All authors reviewed and approved the final manuscript.

Notes

The authors declare no competing financial interest.

ABBREVIATIONS

A2M, alpha-2 macroglobulin; AcSp, aciniform spidroin; APE, Analysis of Phylogenetics and Evolution; ASG, aggregate spider glues; BLAST, Basic Local Alignment Search Tool; C, carboxyl; CEH, carboxyl ester hydrolase; CRP, cysteine-rich protein; Cuticle, cuticle protein; ECP, egg case protein; EDTA, ethylenediaminetetraacetic acid; FMO3, dimethylaniline monooxygenase; GT, glutamyltranspeptidase; HDC, histidine decarboxylase; Hemo_D, hemocyanin subunit D; kb, kilobase; Lectin, putative lectin; *L. hesperus*, *Latrodectus hesperus*; LC−MS/MS, liquid chromatography−tandem mass spectrometry; LTQ, linear trap quadropole; MaSp, major ampullate spidroin; MiSp, minor ampullate spidroin; Mur89F, mucin related 89F; N, amino; NCBI, National Center for Biotechnology Information; PTL, pancreatic triacylglycerol lipase; Scaffold ID no., Scaffold predicted protein number; SDS-PAGE, sodium dodecyl sulfate polyacrylamide gel electrophoresis; SSC, sodium salt citrate; SST, silk-gland specific transcript; TuSp, tubuliform spidroin; UniProt, Universal Protein Resource

REFERENCES

(1) Guerette, P. A.; Ginzinger, D. G.; Weber, B. H.; Gosline, J. M. Silk Properties Determined by Gland-specific Expression of a Spider Fibroin Gene Family. *Science* **1996**, 272 (5258), 112−115.

(2) Gatesy, J.; Hayashi, C.; Motriuk, D.; Woods, J.; Lewis, R. Extreme Diversity, Conservation, and Convergence of Spider Silk Fibroin Sequences. *Science* **2001**, 291, 2603−2605.

(3) Gosline, J. M.; Guerette, P. A.; Ortlepp, C. S.; Savage, K. N. The Mechanical Design of Spider Silks: From Fibroin Sequence to Mechanical Function. *J. Exp. Biol.* **1999**, *202*, 3295−3303.

(4) Vollrath, F.; Knight, D. P. Liquid Crystalline Spinning of Spider Silk. *Nature* **2001**, *410*, 541−548.

(5) Jenkins, J. E.; Holland, G. P.; Yarger, J. L. High Resolution Magic Angle Spinning NMR Investigation of Silk Protein Structure within Major Ampullate Glands of Orb Weaving Spiders. *Soft Matter* **2012**, *8*, 1947−1954.

(6) Jenkins, J. E.; Creager, M. S.; Butler, E. B.; Lewis, R. V.; Yarger, J. L.; Holland, G. P. Solid-state NMR Evidence for Elastin-like *β*-turn Structure in Spider Dragline Silk. *Chem. Commun.* **2010**, *46*, 6714−6716.

(7) Trancik, J. E.; Czernuszka, J. T.; Bell, F. I.; Viney, C. Nanostructural Features of a Spider Dragline Silk as Revealed by Electron and X-ray Diffraction Studies. *Polymer* **2006**, *47*, 5633−5642.

(8) Gould, S. A. C.; Tran, K. T.; Spagna, J. C.; Moore, A. M. F.; Shulman, J. B. Short and Long Range Order of the Morphology of Silk from *Latrodectus hesperus* (Black Widow) as Characterized by Atomic Force Microscopy. *Int. J. Biol. Macromol.* **1999**, *24*, 151−157.

(9) Candelas, G. C.; Cintron, J. A. Spider Fibroin and Its Synthesis. *J. Exp. Zool.* **1981**, *216*, 1−6.

(10) Prince, J. T.; McGrath, K. P.; DiGirolamo, C. M.; Kaplan, D. L. Construction, Cloning, and Expression of Synthetic Genes Encoding Spider Dragline Silk. *Biochemistry* **1995**, *34*, 10879−10885.

(11) Lewis, R. V.; Hinman, M.; Kothakota, S.; Fournier, M. J. Expression and Purification of a Spider Silk Protein: A New Strategy for Producing Repetitive Proteins. *Protein Expression Purif.* **1996**, *7*, 400−406.

(12) Rising, A.; Widhe, M.; Johansson, J.; Hedhammar, M. Spider Silk Proteins: Recent Advances in Recombinant Production, Structure−function Relationships and Biomedical Applications. *Cell. Mol. Life Sci.* **2011**, *68*, 169−184.

(13) Tokareva, O.; Michalczechen-Lacerda, V. A.; Rech, E. L.; Kaplan, D. L. Recombinant DNA Production of Spider Silk Proteins. *Microbial Biotechnology* **2013**, *6*, 651−663.

(14) Work, R. W. Web Components Associated with the Major Ampullate Silk Fibers of Orb-web-building Spiders. *Trans. Am. Microsc. Soc.* **1981**, *100*, 1−20.

(15) Garb, J. E.; Ayoub, N. A.; Hayashi, C. Y. Untangling Spider Silk Evolution with Spidroin Terminal Domains. *BMC Evol. Biol.* **2010**, *10*, 243.

(16) Lane, A.; Hayashi, C. Y.; Whitworth, G. B.; Ayoub, N. A. Complex Gene Expression in the Dragline Silk Producing Glands of the Western Black Widow (*Latrodectus hesperus*). *BMC Genomics* **2013**, *14*, 846.

(17) Andersson, M.; Holm, L.; Ridderstråle, Y.; Johansson, J.; Rising, A. Morphology and Composition of the Spider Major Ampullate Gland and Dragline Silk. *Biomacromolecules* **2013**, *14*, 2945−2952.

(18) Lawrence, B. A.; Vierra, C. A.; Moore, A. M. F. Molecular and Mechanical Properties of Major Ampullate Silk of the Black Widow Spider, *Latrodectus hesperus*. *Biomacromolecules* **2004**, *5*, 689−695.

(19) Ayoub, N. A.; Garb, J. E.; Tinghitella, R. M.; Collin, M. A.; Hayashi, C. Y. Blueprint for a High-performance Biomaterial: Full-length Spider Dragline Silk Genes. *PLoS One* **2007**, *2*, e514.

(20) Ayoub, N. A.; Hayashi, C. Y. Multiple Recombining Loci Encode MaSp1, the Primary Constituent of Dragline Silk, in Widow Spiders (Latrodectus: Theridiidae). *Mol. Biol. Evol.* **2008**, *25*, 277−286.

(21) Colgin, M. A.; Lewis, R. V. Spider Minor Ampullate Silk Proteins Contain New Repetitive Sequences and Highly Conserved Non-silk-like "Spacer Regions. *Protein Sci.* **1998**, *7*, 667−672.

(22) Chen, G.; Liu, X.; Zhang, Y.; Lin, S.; Yang, Z.; Johansson, J.; Rising, A.; Meng, Q. Full-length Minor Ampullate Spidroin Gene Sequence. *PLoS One* **2012**, *7*, e52293.

(23) La Mattina, C.; Reza, R.; Hu, X.; Falick, A. M.; Vasanthavada, K.; McNary, S.; Yee, R.; Vierra, C. A. Spider Minor Ampullate Silk Proteins are Constituents of Prey Wrapping Silk in the Cob Weaver *Latrodectus hesperus*. *Biochemistry* **2008**, *47*, 4692−4700.

(24) Bond, J. E.; Garrison, N. L.; Hamilton, C. A.; Godwin, R. L.; Hedin, M.; Agnarsson, I. Phylogenomics Resolves a Spider Backbone Phylogeny and Rejects a Prevailing Paradigm for Orb Web Evolution. *Curr. Biol.* **2014**, *24*, 1765−1771.

(25) Dimitrov, D.; Lopardo, L.; Giribet, G.; Arnedo, M. A.; Alvarez-Padilla, F.; Hormiga, G. Tangled in a Sparse Spider Web: Single Origin of Orb Weavers and Their Spinning Work Unravelled by Denser Taxonomic Sampling. *Proc. R. Soc. London, Ser. B* **2012**, *279*, 1341−1350.

(26) Garb, J. E.; Hayashi, C. Y. Modular Evolution of Egg Case Silk Genes Across Orb-weaving Spider Superfamilies. *Proc. Natl. Acad. Sci. U. S. A.* **2005**, *102*, 11379−11384.

(27) Tian, M.; Lewis, R. V. Molecular Characterization and Evolutionary Study of Spider Tubuliform (Eggcase) Silk Protein. *Biochemistry* **2005**, *44*, 8006−8012.

(28) Hu, X.; Kohler, K.; Falick, A. M.; Moore, A. M. F.; Jones, P. R.; Sparkman, O. D.; Vierra, C. Egg Case Protein-1: A New Class of Silk Proteins with Fibroin-like Properties from the Spider *Latrodectus hesperus*. *J. Biol. Chem.* **2005**, *280*, 21220−21230.

(29) Hu, X.; Kohler, K.; Falick, A. M.; Moore, A. M. F.; Jones, P. R.; Vierra, C. Spider Egg Case Core Fibers: Trimeric Complexes Assembled from TuSp1, ECP-1, and ECP-2. *Biochemistry* **2006**, *45*, 3506−3516.

(30) Casem, M. L.; Collin, M. A.; Ayoub, N. A.; Hayashi, C. Y. Silk Gene Transcripts in the Developing Tubuliform Glands of the Western Black Widow, *Latrodectus hesperus*. *J. of Arachnol.* **2010**, *38*, 99−103.

(31) Starrett, J.; Garb, J. E.; Kuelbs, A.; Azubuike, U. O.; Hayashi, C. Y. Early Events in the Evolution of Spider Silk Genes. *PLoS One* **2012**, *7*, e38084.

(32) Pham, T.; Chuang, T.; Lin, A.; Joo, H.; Tsai, J.; Crawford, T.; Zhao, L.; Williams, C.; Hsia, Y.; Vierra, C. Dragline Silk: a Fiber Assembled with Low-molecular-weight Cysteine-rich Proteins. *Biomacromolecules* **2014**, *15*, 4073−4081.

(33) Prosdocimi, F.; Bittencourt, D.; da Silva, F. R.; Kirst, M.; Motta, P. C.; Rech, E. L. Spinning Gland Transcriptomics from Two Main Clades of Spiders (order: Araneae)–Insights on Their Molecular, Anatomical and Behavioral Evolution. *PLoS One* **2011**, *6*, e21634.

(34) Clarke, T. H.; Garb, J. E.; Hayashi, C. Y.; Haney, R. A.; Lancaster, A. K.; Corbett, S.; Ayoub, N. A. Multi-tissue Transcriptomics of the Black Widow Spider Reveals Expansions, Co-options, and Functional Processes of the Silk Gland Gene Toolkit. *BMC Genomics* **2014**, *15*, 365.

(35) Sanggaard, K. W.; Bechsgaard, J. S.; Fang, X.; Duan, J.; Dyrlund, T. F.; Gupta, V.; Jiang, X.; Cheng, L.; Fan, D.; Feng, Y.; et al. Spider Genomes Provide Insight into Composition and Evolution of Venom and Silk. *Nat. Commun.* **2000**, *5*, 3765.

(36) Vasanthavada, K.; Hu, X.; Falick, A. M.; La Mattina, C.; Moore, A. M.; Jones, P. R.; Yee, R.; Reza, R.; Tuton, T.; Vierra, C. Aciniform Spidroin, a Constituent of Egg Case Sacs and Wrapping Silk Fibers from the Black Widow Spider *Latrodectus hesperus*. *J. Biol. Chem.* **2007**, *282*, 35088−35097.

(37) Blasingame, E.; Tuton-Blasingame, T.; Larkin, L.; Falick, A. M.; Zhao, L.; Fong, J.; Vaidyanathan, V.; Visperas, A.; Geurts, P.; Hu, X.; La Mattina, C.; Vierra, C. Pyriform Spidroin 1, a Novel Member of the Silk Gene Family That Anchors Dragline Silk Fibers in Attachment Discs of the Black Widow Spider, *Latrodectus hesperus*. *J. Biol. Chem.* **2009**, *284*, 29097−29108.

(38) Jeffery, F.; La Mattina, C.; Tuton-Blasingame, T.; Hsia, Y.; Gnesa, E.; Zhao, L.; Franz, A.; Vierra, C. Microdissection of Black Widow Spider Silk-producing Glands. *J. Visualized Exp.* **2011**, e2382.

(39) Work, R. W.; Emerson, P. D. An Apparatus and Technique for the Forcible Silking of Spiders. *J. Arachnol.* **1982**, *10*, 1−10.

(40) Andon, N. L.; Hollingworth, S.; Koller, A.; Greenland, A. J.; Yates, J. R., III; Haynes, P. A. Proteomic Characterization of Wheat Amyloplasts Using Identification of Proteins by Tandem Mass Spectrometry. *Proteomics* **2002**, *2*, 1156−1168.

(41) Keller, A.; Nesvizhskii, A. I.; Kolker, E.; Aebersold, R. Empirical Statistical Model to Estimate the Accuracy of Peptide Identifications

Made by MS/MS and Database Search. *Anal. Chem.* **2002**, *74*, 5383−5392.

(42) Qian, W. J.; Liu, T.; Monroe, M. E.; Strittmatter, E. F.; Jacobs, J. M.; Kangas, L. J.; Petritis, K.; Camp, D. G.; Smith, R. D. Probability-based Evaluation of Peptide and Protein Identifications from Tandem Mass Spectrometry and SEQUEST Analysis: the Human Proteome. *J. Proteome Res.* **2005**, *4*, 53−62.

(43) Eng, J. K.; McCormack, A. L.; Yates, J. R. An Approach to Correlate Tandem Mass Spectral Data of Peptides with Amino Acid Sequences in a Protein Database. *J. Am. Soc. Mass Spectrom.* **1994**, *5*, 976−989.

(44) *R: A Language and Environment for Statistical Computing*; R Foundation for Statistical Computing: Vienna, Austria, 2014. http://www.R-project.org/.

(45) Paradis, E.; Claude, J.; Strimmer, K. APE: Analyses of Phylogenetics and Evolution in R language. *Bioinformatics* **2004**, *20*, 289−290.

(46) Meyer D.; Buchta, C. Proxy: Distance and Similarity Measures. *R package*, version 0.4-14; R Foundation for Statistical Computing: Vienna, Austria, 2015. http://CRAN.R-project.org/package=proxy.

(47) Micallef, L.; Rodgers, P. eulerAPE: Drawing Area-proportional 3-Venn Diagrams Using Ellipses. *PLoS One* **2014**, *9*, e101717.

(48) Ayoub, N. A.; Garb, J. E.; Kuelbs, A.; Hayashi, C. Y. Ancient Properties of Spider Silks Revealed by the Complete Gene Sequence of the Prey-Wrapping Silk Protein (AcSp1). *Mol. Biol. Evol.* **2013**, *30*, 589−601.

(49) Choresh, O.; Bayarmagnai, B.; Lewis, R. V. Spider Web Glue: Two Proteins Expressed from Opposite Strands of the Same DNA Sequence. *Biomacromolecules* **2009**, *10*, 2852−2856.

(50) Benjamin, S. P.; Zschokke, S. Untangling the Tangle-web: Web Construction Behavior of the Comb-footed Spider *Steatoda triangulosa* and Comments on Phylogenetic Implications (Araneae: Theridiidae). *J. Insect Behav.* **2002**, *15*, 791−809.

(51) Blackledge, T. A.; Summers, A. P.; Hayashi, C. Y. Gumfooted Lines in Black Widow Cobwebs and the Mechanical Properties of Spider Capture Silk. *Zoology* **2005**, *108*, 41−46.

(52) Davies, G. J.; Knight, D. P.; Vollrath, F. Chitin in the Silk Gland Ducts of the Spider *Nephila edulis* and the Silkworm *Bombyx mori*. *PLoS One* **2013**, *8*, e73225.

(53) Vizcaíno, J. A.; Deutsch, E. W.; Wang, R.; Csordas, A.; Reisinger, F.; Ríos, D.; Dianes, J. A.; Sun, Z.; Farrah, T.; Bandeira, N.; Binz, P. A.; Xenarios, I.; Eisenacher, M.; Mayer, G.; Gatto, L.; Campos, A.; Chalkley, R. J.; Kraus, H. J.; Albar, J. P.; Martinez-Bartolomé, S.; Apweiler, R.; Omenn, G. S.; Martens, L.; Jones, A. R.; Hermjakob, H. ProteomeXchange Provides Globally Co-ordinated Proteomics Data Submission and Dissemination. *Nat. Biotechnol.* **2014**, *30*, 223−226.